Characterization of QT-interval adaptation time lag in response to sport-induced heart rate changes measured from wearable ECG recordings

Sofia Romagnoli, Agnese Sbrollini, *Member, IEEE*, Laura Burattini, *Member, IEEE*, Juan Pablo Martínez, and Pablo Laguna, *Fellow, IEEE*

***Abstract*— *Objectives:* Elevated heterogeneity in ventricular repolarization can promote malignant ventricular arrhythmias. During exercise, distinct ventricular cells may present different repolarization adaptation to heart-rate (HR) changes potentially increasing ventricular repolarization dispersion. An electrocardiographic descriptor of the temporal adaptation of action potential duration to HR changes is the time delay the QT interval takes in accommodating to abrupt acceleration and deceleration in HR. Previous investigations have been performed on standard electrocardiograms acquired during stress tests. The present work aims to characterize the time delay of QT-interval accommodation to HR changes for a healthy trained population during real training. *Methods:* The time delay was estimated through an optimally derived, model-based time-delay estimator as the lag between the actual QT series and an HR-derived expected memoryless QT series. The last one was obtained by fitting a logarithmic regression model to the instantaneous QT and HR measurements in assumed stationary time windows. The QT lag was estimated separately in HR acceleration, and HR deceleration, of single-lead ECG acquired through a chest strap while practicing sport. *Results:* The QT-adaptation time lag estimated during HR deceleration is longer than during HR acceleration, especially after intense physical exertion of athletes when they have overcome their theoretical maximal HR 14.5[2.4;28.0] s or they have been involved in dynamic sports 9.9[5.8;24.9] s. *Conclusion:* Higher repolarization dispersion can be captured by the proposed time delay biomarker in a distinctive way to the HR acceleration. *Significance:* Eventually the time lag is a biomarker for exacerbated increase of ventricular repolarization dispersion while exercising.**

***Index Terms*—Electrocardiogram, QT-RR delay, Sport, Sudden Cardiac Death, Wearable sensor**

I. Introduction

Sudden cardiac death (SCD) is defined as death presumed to be of a cardiac cause that occurs within 1 hour of the onset of cardiac symptoms or 24 hours of last being seen healthy and alive. SCD may be the first presentation of cardiovascular diseases and it accounts for half of cardiovascular deaths [1]. Intense exercise may impact the risk of suffering SCD in individuals with underlying unknown cardiac abnormalities [2], [3]. Sport-related SCD is an unexpected death occurring while practicing a sport activity, after exercise at rest within one hour from its cessation or during sleep [2], [3]. When occurring in athletes under 35 years old, it is considered independent from other age-influenced cardiovascular complications [2], [3].

Prevention remains the major weapon to reduce the occurrence of sport-related SCD [4]. A large variety of non-invasive electrocardiographic biomarkers for arrhythmic risk stratification was proposed to prevent malignant ventricular arrhythmias.

The initiation and maintenance of ventricular arrhythmias depend on three main factors: substrate, triggers, and modulators. A vulnerable myocardium is the substrate for arrhythmogenesis, meaning that when triggering factors appear, they can lead to malignant arrhythmias potentially ending in SCD [5]. Elevated repolarization heterogeneity in the ventricular myocardium among different ventricular myocardial cells or regions has been identified as a characteristic of a vulnerable substrate [6]. During exercise, ventricular repolarization dispersion can be exacerbated in response to changes in heart rate (HR) due to the different repolarization adaptation to HR changes presented by distinct ventricular cells [7]. An important modulator of arrhythmogenic substrate is the autonomic nervous system (ANS). Sympathetic nervous system hyperactivity has been shown to increase triggered activity and enhance dispersion of ventricular repolarization thus enhancing vulnerability to ventricular arrhythmias [8], [9]. In addition to spatial heterogeneities, increased temporal repolarization heterogeneities, associated to the abnormal adaptation of action potential duration to HR changes, have been linked to vulnerable substrate [5].

Multiple studies have challenged the identification of descriptors of the temporal heterogeneity in repolarization measured from the surface electrocardiogram (ECG) as potential biomarkers of arrhythmic risk. Among those, one seemingly promising repolarization descriptor is the time of accommodation of the QT interval to HR changes, referred to as QT/RR hysteresis[9], [10], [11], [12], [13], [14]. Hysteresis in the electrical cardiac activity is given by the time delay in the adaptation of action potential morphology to RR-interval changes [15]. The hysteresis is actually understood to increase

Manuscript submitted on July 4, 2024. The work was supported by projects PID2022-140556OB-I00, and TED2021-130459B-I00 funded by Spanish Ministry of Science and Innovation (MICINN) and FEDER, by Gobierno de Aragón (Reference Group Biomedical Signal Interpretation and Computational Simulation (BSICoS) T39_23R. The computation was performed at the High Performance computing platform of the NANBIOSIS ICTS *(Corresponding author: Sofia Romagnoli, (sromagnoli@unizar.es)).*

S. Romagnoli, J.P. Martínez, and P. Laguna are with the Biomedical Signal Interpretation & Computational Simulation Group (BSICoS), Aragón Institute of Engineering Research (I3A), Zaragoza University, Zaragoza, and CIBER-BBN, Spain. A. Sbrollini and L. Burattini are with the Department of Information Engineering of Università Politecnica delle Marche, Italy.

electrical stability by facilitating ventricular filling/emptying and the coronary perfusion [16]. Thus, the QT/RR hysteresis represents how fast the QT interval attains its steady-state following a sustained variation in RR interval. Instead, in a steady-state condition, the dynamic QT/RR relationship is represented by the QT on RR parametric dependency, which characterizes how much the steady-state QT interval varies in function of the steady-state RR intervals. Thus, the relation between HR changes and their induced QT changes has been modelled with a memoryless transformation (typically non-linear), representing the stationary relation between QT with RR, followed by a first order linear system representing the system memory [11], [13], [14].

The QT/RR hysteresis can be invasively induced by atrial and ventricular pacing using varying protocols, e.g., atropine injection [16]. Although, the most obvious manifestation of QT/RR hysteresis is the differential response of the QT interval during sequential HR acceleration and deceleration during exercise and recovery. Abrupt HR changes can be induced during exercise stress tests, where QT-time lag can be measured. HR presents a linear-trend variation in stress tests, and the QT series should then follow the HR changes with another similar trend delayed by the time lag under estimation [13]. The time delay of QT-interval values in following changes in the HR values was computed as the time lag between the observed QT series and an expected instantaneous memoryless HR-dependent QT series, derived from the HR and a patient-specific model of the QT on RR dependency [13]. This method was clinically evaluated in stress tests from patients with suspected cardiovascular disease, to characterize arrhythmias and SCD risk focusing on the standard ECG acquired in clinical setting during stress tests [13]. Moreover, a validation of QT time-lag estimation has also been performed in a controlled simulated experiment[17]. Longer QT-hysteresis lags have been associated with abnormal temporal repolarization heterogeneities [13].

The application of this method to monitor the cardiac activity during real exercise is also potentially important because it can shed light on what happens with cardiac electrophysiology during physical activity when malignant arrhythmogenic events may occur, especially in subjects with congenital or structural heart diseases. Although, ECGs during physical activity are characterized by a low signal to noise ratio (SNR), making the analysis of RR and QT intervals challenging. Thus, the primary aim of the present work is to adapt this method for computation of the QT-interval time lag in accommodating to HR changes to single-lead ECG recordings acquired during free exercise in a real-life scenario, and evaluate its potential to estimate the QT-adaptation time both during HR acceleration and HR deceleration of the sport. This will allow to estimate the QT-adaptation time from wearable-derived ECG acquired while practicing sports, allowing continuous cardiac monitoring of athletes. The study is performed on a healthy trained population. A preliminary methodological version of this work has been reported [18].

TABLE I: Database numerousness: number of athletes involved in the study together with the practiced sports and number of cardiorespiratory sets composing each database. Numbers in parenthesis indicate the numbers of analysed ECGs after exclusions described in sections III-B and III-H.

Database	**Sport**	**# Athletes**	**# Signal sets**	
			available	usable
SPDB	Aerial silk	3	3	(2)
	Basketball	9	9	(5)
	Crossfit	19	28	(10)
	Fitness	8	8	(5)
	Jogging	5	19	(1)
	Middle distance race	10	10	(5)
	Running	10	10	(8)
	Soccer	2	14	(0)
	Tennis	9	19	(2)
	Zumba	6	6	(0)
	All sports	81	126	(38)
SPDB2	Running	10	10	(10)
	Cycling	12	12	(2)
	All sports	22	22	(12)

II. Materials

Analysed ECGs are part of two databases belonging to Cardiovascular Bioengineering Lab of Università Politecnica delle Marche: Sport DB (SPDB) and Sport DB 2.0 (SPDB2) [19], [20]. Cardiorespiratory recordings contained in the databases were acquired through the wearable sensor BioHarness 3.0 by Zephyr (https://www.zephyranywhere.com/). Each subject may have been recorded at more than one training session, each training constituting a set of signals. In these cases, only the datasets with the highest SNR (refer to section III-B) is analysed. Each set of analysed cardiorespiratory signals contains a single-lead ECG sampled at a sampling rate $F_s = 250$ Hz. All cardiorespiratory recordings are continuous recordings acquired in real-life uncontrolled condition on the training field. The acquisition protocol includes three phases: pre-exercise resting, exercise and post-exercise resting. The pre-exercise resting consists in lying or sitting courtside for at least 5 minutes; the exercise phase has free duration and athletes are following their own training protocol; the recovery phase usually coincides with stretching or sitting courtside for at least 5 minutes.

The 20 datasets belonging to subjects practicing soccer and Zumba do not contain the ECG. Furthermore, one subject practicing tennis with paroxysmal atrial fibrillation (11 datasets) presented episodes of no sinus rhythm during the recording and it was excluded from the analysis. A subject practicing jogging has short QT syndrome (SQTS). The 5 datasets belonging to this subject were analysed and reported separately as a case report. Thus, from the 148 available cardiorespiratory signal sets, only 50 ECG belonging to 50 healthy athletes are analysed. The numerousness of the databases before and after application of ECGs exclusion criteria (refer to sections III-B and III-H) is reported in Table I.

III. Methods

The main methodological steps needed to estimate the time delay of QT series in following HR changes are displayed in Fig. 1. Delineation of electrocardiographic waves and ECG

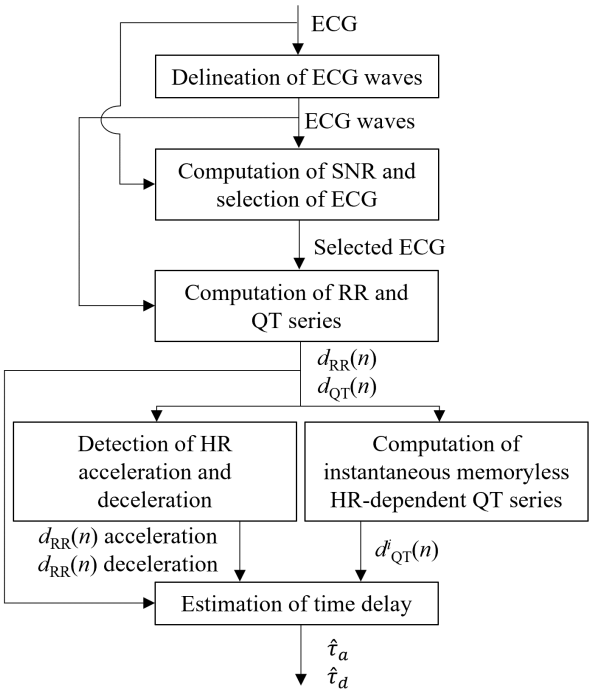

Fig. 1: Block scheme of the methodological steps to estimate the time delay between QT-interval series and the RR series.$\hat{\tau}_a$ denotes the time delay estimated during HR acceleration, and $\hat{\tau}_d$ denotes the time delay estimated during HR deceleration.

processing are the first steps. After rejection of noisy areas based on signal to noise ratio (SNR) rules, RR $(d_{\mathrm{RR}}(n))$ and QT $(d_{\mathrm{QT}}(n))$ series are generated. An instantaneous memoryless, HR dependent, QT series $(d^i_{\mathrm{QT}}(n))$ is estimated. This step is followed by the identification of HR acceleration and HR deceleration where the QT-adaptation time lag is estimated as the delay between $d_{\mathrm{QT}}(n)$ and $d^i_{\mathrm{QT}}(n)$ series.

A. ECG waves delineation

QRS detection and ECG-waves delineation was done through a single-lead wavelet-based algorithm [21]. Delineation of ECG waves was performed using a wavelet-transform-based delineator [21], which identifies local maxima, minima and zero-crossings in the signal derivatives at different scales. The T-wave end is assigned to the sample where the signal derivative falls below a threshold relative to the maximum derivative of the T-wave final slope.

ECG recordings from wearable recorders have large inter-sport disparity in amplitude ranges which were not originally contemplated in the design of the detector. To circumvent that limitation each ECG was first segmented in excerpt lasting 60 s and scaled in amplitude to have interquartile amplitude range of 1 mV. The annotations of wave delineation were visually inspected. In areas with large number of false negative wave detection due to artifacts represented by high amplitude spikes, the ECG excerpts were further segmented in smaller windows excluding artifacts. Those ECG windows were analysed again through the single-lead detector [21] and the newly delineated waves were the marks used in subsequent steps.

B. Signal to noise ratio estimation and ECG excerpt selection

In practice, the quality of ECG recordings during exercise is negatively affected by exercise-related artifacts which make electrocardiographic measures unreliable in signal excerpts having very large noise contamination. Two different noise types are common in exercise ECGs: high-frequency (HF) noise, mainly due to muscle activity, and low-frequency (LF) noise due to baseline wander. To identify, and discard from the analysis, those areas highly contaminated by these types of noise, a high-frequency SNR, ($\mathrm{SNR_{HF}}$) and a low-frequency SNR ($\mathrm{SNR_{LF}}$) are defined and estimated to determine the quality of ECG [22].

First, ECG signal excerpts of 60 s are taken and their cardiac beats are segmented. The length of each cardiac beat segmentation window is taken HR-dependent. The onset (n_o) and end (n_e) time instants of the HR-dependent beat interval, referred to the k-th QRS-complex mark (n_r) provided by the QRS detector, are computed as in [23]:

$$n_o(k) = n_r(k) - 0.240F_s, \tag{1}$$

representing 240 ms ahead of the QRS mark, and

$$n_e(k) = \begin{cases} n_r(k) + \frac{2}{3}\overline{\mathrm{RR}}F_s & \overline{\mathrm{RR}} < 0.720 \text{ s} \\ n_r(k) + \min\{0.684, \overline{\mathrm{RR}} - 0.240\}F_s & \overline{\mathrm{RR}} \geq 0.720 \text{ s} \end{cases}, \tag{2}$$

where $\overline{\mathrm{RR}}$ is the mean of RR intervals (in seconds) in ECG excerpt of 60 s.

The $\mathrm{SNR_{HF}}$ of the k-th beat is defined as the ratio of the peak-to-peak amplitude of the cardiac beat, and the root-mean-square (RMS) value of its HF noise, computed after Butterworth high-pass filtering with cut-off frequency $F_c = 20$ Hz, in an HR-dependent interval with onset at $n_r(k) + 0.148F_s$ (148 ms after the k-th QRS mark) and end at $n_e(k)$ [22].

The $\mathrm{SNR_{LF}}$ at each beat is defined as the ratio of the peak-to-peak amplitude of the average beat over the 60 s excerpt ECG and the RMS value of the residual ECG after average beat subtraction and low-pass filtering using a Butterworth filter with $F_c = 20$ Hz [22]. Beats were aligned before averaging by maximizing cross-correlation between each beat and a median reference beat computed from those with correlation coefficient ≥ 0.8 within the excerpt.

For each ECG excerpt, median $\mathrm{SNR_{HF}}$ $(\mathrm{SNR^m_{HF}})$ and $\mathrm{SNR_{LF}}$ $(\mathrm{SNR^m_{LF}})$ across beats were computed. If $\mathrm{SNR^m_{HF}} > 40$ and $\mathrm{SNR^m_{LF}} > 3$, the ECG excerpt was considered of sufficient quality for further processing. If the percentage of excerpts in the recording, labeled as of sufficient quality is >65%, the ECG is considered for RR and QT-series computation. Otherwise, the entire recording is discarded. Furthermore, even if the ECG is considered acceptable, the QT changes episodes that belongs to ECG excepts with $\mathrm{SNR^m_{HF}} < 40$ or $\mathrm{SNR^m_{LF}} < 3$ were discarded from further analysis.

C. Estimation of RR and QT series

The RR-interval series $d_{\mathrm{RR}}(k)$, is computed from the k-th QRS-complex mark as

$$d_{\mathrm{RR}}(k) = \frac{n_r(k) – n_r(k–1)}{F_s}. \tag{3}$$

Analogously, the QT-interval series $d_{\mathrm{QT}}(k)$, [10] is computed as

$$d_{\mathrm{QT}}(k) = \frac{n_{\mathrm{T_e}}(k) - n_{\mathrm{QRS_o}}(k)}{F_s}, \tag{4}$$

where $n_{\mathrm{T_e}}(k)$ and $n_{\mathrm{QRS_o}}(k)$ are the T-wave end and QRS-complex onset samples of the k-th cardiac beat respectively. Missing values in the series were linearly interpolated [13]. Outlier values of both $d_{\mathrm{RR}}(k)$ and $d_{\mathrm{QT}}(k)$ series, identified as those deviating by more than ±10% or ±5%, respectively, from the running median of each series computed over 40 beats were replaced with the corresponding median value. Subsequently, $d_{\mathrm{RR}}(k)$ and $d_{\mathrm{QT}}(k)$ series were piecewise cubic Hermite interpolated to 4 Hz with, becoming uniformly sampled time series, $d_{\mathrm{RR}}(n)$ and $d_{\mathrm{QT}}(n)$ [13].

D. Expected instantaneous memoryless HR-dependent QT

To estimate the time lag of the $d_{\mathrm{QT}}(n)$ series following the $d_{\mathrm{RR}}(n)$ series, the expected instantaneous memoryless HR-dependent QT-interval series $d^i_{\mathrm{QT}}(n)$ was estimated. The $d^i_{\mathrm{QT}}(n)$ series contains the QT values that would correspond to each $d_{\mathrm{RR}}(n)$ if the HR at that point was stationary. A logarithmic regression model was used to compute $d^i_{\mathrm{QT}}(n)$[11].

$$d^i_{\mathrm{QT}}(n) = \beta + \alpha \ln(d_{\mathrm{RR}}(n)). \tag{5}$$

The values of the parameters β and α for the logarithmic regression model in (5) were obtained by fitting [$d_{\mathrm{QT}}(n)$, $d_{\mathrm{RR}}(n)$] data pairs taken from different HR-stationary ECG signal excerpts, simultaneously. Stationarity of $d_{\mathrm{RR}}(n)$ was continuously evaluated through the ratio ($\mathcal{R}$) between the standard deviation, σ_{RR}, and the mean, $\overline{\mathrm{RR}}$, of $d_{\mathrm{RR}}(n)$ series,

$$\mathcal{R} = \frac{\sigma_{\mathrm{RR}}}{\overline{\mathrm{RR}}}, \tag{6}$$

in a moving window of 30 s with 15 s overlap. If $\mathcal{R} < 0.05$ the last 15 s of the window is considered as eligible stationary signal excerpt for model parameter estimation. To be sure that representative data from the maximum possible amplitude excursion of $d_{\mathrm{RR}}(n)$ is considered, six stationary excerpts which $\overline{\mathrm{RR}}$ is closest to the maximum, minimum and mean (two windows from each condition) value of $d_{\mathrm{RR}}(n)$ in the complete record, were considered as data segments for model parameter estimation.

The values of $d_{\mathrm{RR}}(n)$ and $d_{\mathrm{QT}}(n)$ are assumed to be stationary in these windows and representative of the subject instantaneous QT on RR dependency. Model parameters were estimated using least squares minimization with these data. A least-squares fit of the [$d_{\mathrm{QT}}(n)$, $d_{\mathrm{RR}}(n)$] data pairs was performed and patient-specific values of $\hat{\alpha}$ and $\hat{\beta}$ were obtained. The resulting minimum root mean square error,

$$\epsilon = \sqrt{\frac{1}{6 \times 15 \times 4} \sum_{\substack{n \in \{W_j\} \\ j \in \{1,2,3,4,5,6\}}} \left(d_{\mathrm{QT}}(n) - d^i_{\mathrm{QT}}(n) \right)^2}, \tag{7}$$

of the goodness of fit of the QT-to-RR relationship in the six fitting windows W_j, j$\in \{1, 2, 3, 4, 5, 6\}$, was used to evaluate model fitting.

The expected instantaneous, memoryless, HR-dependent QT-interval series $d^i_{\mathrm{QT}}(n)$, was then calculated all along the recording (not just at the selected windows) following the model in (5) with the estimated $\hat{\alpha}$ and $\hat{\beta}$.

E. Detection of HR acceleration and deceleration episodes by a GLRT-based detector

HR changes during ambulatory recordings, and even more during exercise, generally include acceleration and deceleration transitions, having a ramp-like pattern, representative of episodes of exercising and recovery, respectively. To identify these episodes, characterized by large RR excursion where the QT to RR accommodations is aimed to be estimated, we designed a hypothesis test detector, based on a Generalized Likelihood Ratio Test (GLRT). This detector assumes a linear transition of the RR series between an initial and a final value, which resembles the one described in [24] in the context of ischemia detection based on QRS angle variations, which serves as the basis for the detector here presented.

In the signal model, hypothesis $\mathcal{H}_1$ corresponds to an observed signal where an HR change of length D samples is present, while hypothesis $\mathcal{H}_0$ assumes that the window contains just stationary fluctuations of HR, considered as "noise". The detector models the HR changes as a unitary RR transition in the middle of the window, $h(n)$, $n = 0, ..., D-1$, following a linear trend in an interval of T samples, and then scaled by an amplitude factor $a > 0$ and distorted by noise $w(n)$ with Laplacian distribution (with mean value b and variance σ). For the window starting at $n = n_0$, the signal model is:

$$\left.\begin{array}{ll} \mathcal{H}_0: & d_{\mathrm{RR}}(n) = w(n) \\ \mathcal{H}_1: & d_{\mathrm{RR}}(n) = a h(n - n_0) + w(n) \end{array}\right\} n = n_0, ..., n_0 + D - 1. \tag{8}$$

When the level of exercise increases (transitioning from rest to exercise), $d_{\mathrm{RR}}(n)$ decreases having a negative transient slope $r(n)$ during T even samples corresponding to 30 s, $T = 30 \times 4$, $h(n) = r(n)$. When the level of exercise decreases the change occurs in the opposite direction and $h(n) = -r(n)$. The transient slope model $r(n)$ can be expressed (Fig. 2) as:

$$r(n) = \begin{cases} 1, & n = 0, ..., \frac{D-T}{2} - 1 \\ 1 - \frac{2}{T+1}\left(n - \frac{D-T-2}{2}\right) & n = \frac{D-T}{2}, ..., \frac{D+T}{2} - 1 \\ -1, & n = \frac{D+T}{2}, ..., D - 1 \end{cases}. \tag{9}$$

The Laplacian noise $w(n)$ probability density function (PDF) is:

$$p(w(n)) = \frac{1}{\sqrt{2}\sigma} \exp\left[-\frac{\sqrt{2}}{\sigma} |w(n) - b| \right] \tag{10}$$

with mean b and variance σ^2. The σ value can be estimated based on $d_{\mathrm{RR}}(n)$ PDF in the initial N_σ samples of the recording where exercise has not yet started, obtaining a ML estimate $\hat{\sigma}$ regardless of the hypothesis $\mathcal{H}_0$ or $\mathcal{H}_1$,

$$\hat{\sigma} = \frac{\sqrt{2}}{N_\sigma} \sum_{n=1}^{N_\sigma} \left| d_{\mathrm{RR}}(n) - \hat{b}_\sigma \right|. \tag{11}$$

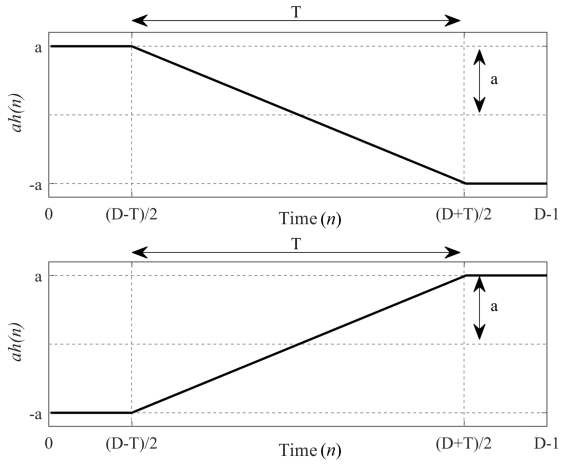

Fig. 2: Ramp-like change $ah(n)$ with a transition of duration T and amplitude factor a, upper panel for HR accelerations, $h(n) = r(n)$, and lower panel for deceleration, $h(n) = -r(n)$.

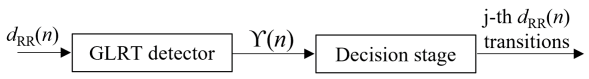

Fig. 3: Block diagram of the method for detection of heart rate acceleration and deceleration using a GLRT-based method.

where $\hat{b}_\sigma = \text{med}\{d_{\text{RR}}(n)\}$, $n \in \{1, \cdots, N_\sigma\}$,

The Laplacian model in (10) is adopted in the present study because the HR variations, $d_{\text{RR}}(n)$, in recordings acquired during sport activities, can contain large number of outliers. These are typically a consequence of false positive and negative QRS detection in low signal-to-noise ratio ECG recordings, even in stationary situations. Consequently better characterized by a Laplacian than a Gaussian PDF, see histograms in Sec.IV-B.

Since the parameters of the above signal model are unknown, the GLRT was used as the basis for HR acceleration and deceleration episodes detection Fig. 3.

The GLRT is the likelihood ratio test between the probabilities associated with the two hypotheses, where the unknown parameter of the signal model, under both hypothesis, are replaced with their maximum likelihood (ML) estimates. Thus, using the Laplacian distribution, the GLRT decides $\mathcal{H}_1$ if:

$$\Lambda^{n_0}(d_{\text{RR}}) = \frac{p(d_{\text{RR}};\ \hat{a}_{\mathcal{H}_1}, \hat{b}_{\mathcal{H}_1}, \mathcal{H}_1)}{p(d_{\text{RR}};\ \hat{b}_{\mathcal{H}_0}, \mathcal{H}_0)} = \frac{\exp\left[-\frac{\sqrt{2}}{\hat{\sigma}} \sum_{n=n_0}^{n_0+D-1} \left| d_{\text{RR}}(n) - \hat{b}_{\mathcal{H}_1} - \hat{a}_{\mathcal{H}_1} h(n-n_0) \right| \right]}{\exp\left[-\frac{\sqrt{2}}{\hat{\sigma}} \sum_{n=n_0}^{n_0+D-1} \left| d_{\text{RR}}(n) - \hat{b}_{\mathcal{H}_0} \right| \right]} > \gamma, \tag{12}$$

where $\hat{a}_{\mathcal{H}_i}$ and $\hat{b}_{\mathcal{H}_i}$ denote the ML estimates of a and b under hypothesis $\mathcal{H}_i$, $i \in \{0, 1\}$. Taking the logarithm of both sides the detector output becomes

$$\Upsilon(n_0) = \ln(\Lambda^{n_0}(d_{\text{RR}})) = \frac{\sqrt{2}}{\hat{\sigma}} \sum_{n=n_0}^{n_0+D-1} \left| d_{\text{RR}}(n) - \hat{b}_{\mathcal{H}_0} \right| - \left| d_{\text{RR}}(n) - \hat{b}_{\mathcal{H}_1} - \hat{a}_{\mathcal{H}_1} h(n-n_0) \right| > \gamma', \tag{13}$$

with $\gamma' = \ln \gamma$. The ML estimates of $\hat{b}_{\mathcal{H}_0}$, $\hat{b}_{\mathcal{H}_1}$ and $\hat{a}_{\mathcal{H}_1}$, derived in [24], [25], can be computed as:

$$\hat{b}_{\mathcal{H}_0} = \text{med}\{d_{\text{RR}}(n)\} \tag{14}$$

$$\hat{b}_{\mathcal{H}_1} = \text{med}\{d_{\text{RR}}(n) - \hat{a}_{\mathcal{H}_1} h(n-n_0)\} \tag{15}$$

$$\hat{a}_{\mathcal{H}_1} = \max\left\{0, \text{med}\left\{ |h(n-n_0)| \diamondsuit \left(\frac{d_{\text{RR}}(n) - \hat{b}_{\mathcal{H}_1}}{h(n-n_0)} \right) \right\}\right\}, \tag{16}$$

all medians computed from values at time interval spanning the complete window under analysis, $n \in \{n_0, ..., n_0 + D - 1\}$. As both ML estimates $\hat{b}_{\mathcal{H}_1}$ and $\hat{a}_{\mathcal{H}_1}$ need to be estimated together, an iterative optimization was applied [25] where an initial estimate of $\hat{b}_{\mathcal{H}_1}$ is taken as the median of $d_{\text{RR}}(n)$. Typically the estimation of $\hat{b}_{\mathcal{H}_1}$ and $\hat{a}_{\mathcal{H}_1}$ converges to stable values in less than 10 iterations.

A test series, $\Upsilon(n)$, can be generated by computing the test $\Upsilon(n_0)$ for each possible value of n_0 in the signal. The threshold γ' is computed as the 75^{th} percentile of the amplitude of $\Upsilon[n]$ in each recording. In order to avoid detection of noise bursts as episodes, a lower limit of 10 s to the width of detected peak in $\Upsilon[n]$ was imposed.

The location of each j-th HR change episodes is then assigned to sample positions, n_j, where $\Upsilon(n)$ test has a maximum which crosses the γ' threshold. Distinction can be made between acceleration and deceleration HR episodes, by applying the detector twice, with $h(n) = r(n)$ for accelerations, and with $h(n) = -r(n)$ for decelerations. Fig. 4 shows $\Upsilon(n)$ example of the GLRT-based detector output for significant accelerations and decelerations episodes.

F. Estimators of QT-adaptation time

The estimation of time delay τ_j between $d_{\text{QT}}(n)$ and $d^i_{\text{QT}}(n)$ series during j-th HR changes can be formulated as a two-channel time delay estimation [26]. To derive the ML time delay estimator we depart from the signal model of the two series as

$$\left.\begin{array}{l} x_1(n) = s(n) + v_1(n) \\ x_2(n) = s(n-\tau) + v_2(n) \end{array}\right\} n = 0, ..., N-1, \tag{17}$$

where $x_1(n)$ and $x_2(n)$ correspond to $d^i_{\text{QT}}(n)$ and $d_{\text{QT}}(n)$, respectively. The observed signal $x_1(n)$ is assumed to be composed of an unknown signal $s(n)$, representing the QT change trend, and additive stationary white noise $v_1(n)$ with variance σ_v^2 (modelled either as Gaussian or as Laplacian). The same assumption applies for the second channel except that the QT trend is delayed by an unknown time τ. It is assumed that the QT trend $s(n)$ has flat (constant) behaviour at the onset and end extremes of the observation window in a duration which guarantees that delaying by τ the series, it

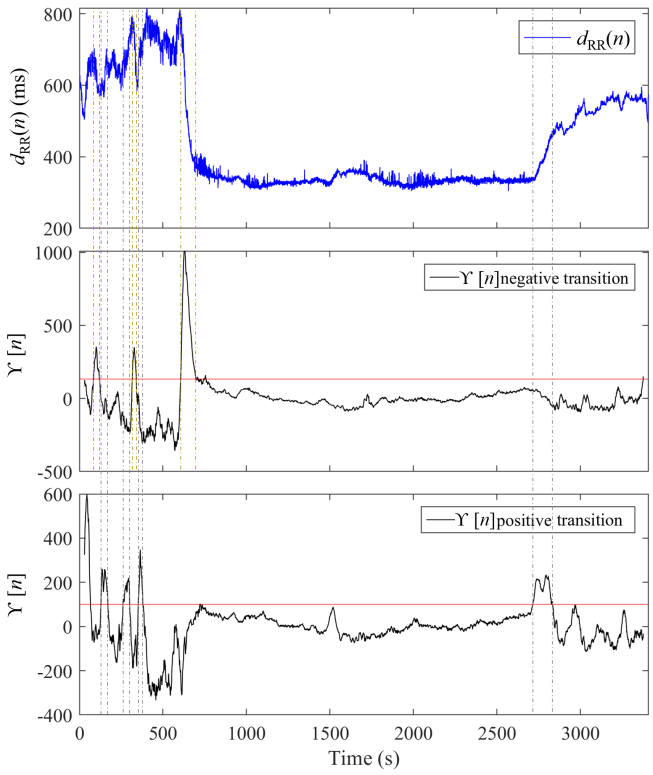

Fig. 4: Example of $d_{\mathrm{RR}}(n)$ series (top panel) together with its GLRT detector $\Upsilon(n)$ series for HR accelerations-induced negative transitions ($h(n) = r(n)$, middle panel), and for HR decelerations-induced positive transitions ($h(n) = -r(n)$, bottom panel). The red line denotes thresholds γ' values.

still has the same flat value at onset and end samples (step transition much shorter than the observation interval).

Thus, the ML time delay estimate of τ will depend on the assumed distribution of the series. The PDF which characterizes the available observation $\mathbf{x}_i = \left[x_i(0) \cdots x_i(N-1)\right]^T$ $i \in \{1,2\}$, with $\mathbf{s} = \left[s(0) \cdots s(N-1)\right]^T$, and assuming $v_1(n)$ and $v_2(n)$ uncorrelated and with Gaussian PDF, results in [26]:

$$p_v(\mathbf{x}_1, \mathbf{x}_2; \tau, \mathbf{s}) = \prod_{n=0}^{N-1} \frac{1}{2\pi\sigma_v^2} \exp\left[-\frac{\big(x_1(n)-s(n)\big)^2+\big(x_2(n)-s(n-\tau)\big)^2}{2\sigma_v^2}\right]. \quad (18)$$

Taking the logarithm and grouping factors independent of τ or $\mathbf{s}$, we obtain

$$\ln p_v(\mathbf{x}_1, \mathbf{x}_2; \tau, \mathbf{s}) = \text{Constant} + -\tfrac{1}{2\sigma_v^2} \sum_{n=0}^{N-1} \Big(\big(x_1(n)-s(n)\big)^2+\big(x_2(n)-s(n-\tau)\big)^2\Big). \quad (19)$$

Maximization of the log-likelihood function in (19) is done by first differentiating with respect to $s(n)$ for a given τ,

$$\frac{\partial \ln p_v(\mathbf{x}_1, \mathbf{x}_2; \tau, \mathbf{s})}{\partial s(n)} = \frac{1}{\sigma_v^2}\big(x_1(n)+x_2(n+\tau)-2s(n)\big), \quad (20)$$

which when set to zero, results in the following estimator for $s(n)$

$$\hat{s}(n;\tau) = \frac{x_1(n) + x_2(n+\tau)}{2}. \quad (21)$$

Inserting $\hat{s}(n;\tau)$ into the log-likelihood function in (19) and maximizing with respect to the other parameter τ, we obtain

$$\hat{\tau} = \arg\min_{\tau}\left(\sum_{\mathrm{n=0}}^{\mathrm{N-1}}\big(\mathrm{x_1(n)-x_2(n+\tau)}\big)^2+\big(\mathrm{x_2(n)-x_1(n-\tau)}\big)^2\right) = \arg\max_{\tau}\left(\frac{1}{2}\sum_{\mathrm{n=0}}^{\mathrm{N-1}}\big(\mathrm{x_1(n)x_2(n+\tau)+x_2(n)x_1(n-\tau)}\big)-\frac{\mathrm{E_x}(\tau)}{4}\right) \quad (22)$$

with

$$E_x(\tau) = \sum_{n=0}^{N-1}\left(x_1^2(n) + x_2^2(n) + x_1^2(n-\tau) + x_2^2(n+\tau)\right). \quad (23)$$

Since the signal $s(n)$ is supposed to have a constant value in intervals larger than τ at the observation window extremes, the estimator in (22), from first equality, is just the least square estimate varying τ,

$$\hat{\tau}^{\mathrm{LS}} = \arg\min_{\tau}\sum_{n=0}^{N-1}\big(x_1(n) - x_2(n+\tau)\big)^2. \quad (24)$$

Alternatively, we know that if $s(n)$ is of finite support (the signal has a finite number of non-zero values) and contained in the observation interval, E_x becomes independent of τ and the ML estimate, from second equality in (22), results in maximizing in τ the cross-correlation between $x_1(n)$ and $x_2(n+\tau)$ [26]. However, since here $s(n)$ is not zero at the interval extremes, and in addition its values can differ from one extreme to the other, $E_x(\tau)$ does depend on τ making the ML estimate resulting from (22) noninterpretable as a cross-correlation maximization. If we rather modify the signals $x_1(n)$, and $x_2(n)$ by adding a constant value b, such that the mean values at the extremes of the new signals, $\tilde{x}_i(n) = x_i(n) - b_i$, $i \in \{1,2\}$, becomes symmetric with same module and reverted sign, we have $E_{\tilde{x}}$ independent of τ and we will obtain the cross-correlation ML estimate but based on the modified signal $\tilde{x}_i(n)$. We can estimate b_i as

$$\hat{\mathrm{b}}_{\mathrm{i}} = \frac{\mathrm{med}\big\{\mathrm{x_i(0),...,x_i(I-1)}\big\} + \mathrm{med}\big\{\mathrm{x_i(N-I),...,x_i(N-1)}\big\}}{2} \quad (25)$$

with I the number of samples at the observation interval onset and end where we have guarantees that the HR is stationary.

The ML estimate is then the one that maximizes the cross-correlation function between the available modified observations,

$$\hat{\tau}^{\mathrm{CC}} = \arg\max_{\tau}\left(\sum_{n=0}^{N-1}\tilde{x}_1(n)\tilde{x}_2(n-\tau)\right); \quad \tau \in \{-I,...,I\}, \quad (26)$$

which, when expressed in terms of the QT series at each j-th HR changes becomes the estimator

$$\hat{\tau}_{\mathrm{j}}^{\mathrm{CC}} = \arg\max_{\tau}\left(\sum_{\mathrm{n=n_{j,o}}}^{\mathrm{n_{j,e}}}\tilde{\mathrm{d}}_{\mathrm{QT}}^{\mathrm{j}}(\mathrm{n})\tilde{\mathrm{d}}_{\mathrm{QT}}(\mathrm{n}-\tau)\right); \tau \in \{-\mathrm{I},...,\mathrm{I}\}, \quad (27)$$

with $n_{j,o}$ and $n_{j,e}$ the onset and end samples, respectively, of the j-th detected HR change episode. $n_{j,o}$ is estimated as the first sample when $\Upsilon(n)$ test crosses threshold γ' backwards

from n_j, and retracting backwards an extra of I samples. Similarly is done for $n_{j,e}$ by searching the crossing forward from n_j and adding an extra I samples forward.

The ML estimators $\hat{\tau}_j^{\text{CC}}$ and $\hat{\tau}_j^{\text{LS}}$ are derived from the assumption of Gaussian noise. However, features derived from the ECG use to be better represented by Laplacian rather than Gaussian distributions, as is the case of QRS angles [24] or Karhunen-Loève transform coefficients from the T wave [25]. The QT interval is a measure based on QRS onset and T end identifications, largely subject to outliers, suggesting the consideration of Laplacian models when estimating the delay between the QT series.

To derive the ML time delay estimation under Laplacian noise distribution we depart from the same signal model in (IV), but now with the Laplacian noise PDF as in (10), resulting in the following observation signals PDF:

$$p_v(\mathbf{x}_1,\mathbf{x}_2;\tau,\mathbf{s}) = \prod_{n=0}^{N-1}\frac{1}{2\sigma_v^2}\exp\left[-\frac{\sqrt{2}}{\sigma_v}\Big(\big|x_1(n)-s(n)\big|+\big|x_2(n)-s(n-\tau)\big|\Big)\right]. \tag{28}$$

Taking the logarithm and grouping factors independent of τ or $\mathbf{s}$, we obtain

$$\ln p_v(\mathbf{x}_1,\mathbf{x}_2;\tau,\mathbf{s}) = \text{Constant}+ -\frac{\sqrt{2}}{\sigma_v}\sum_{n=0}^{N-1}\big(|x_1(n)-s(n)|+|x_2(n)-s(n-\tau)|\big). \tag{29}$$

Maximization of the log-likelihood function in (29) is done by first differentiating with respect to $s(n)$ for a given τ,

$$\frac{\partial \ln p_v(\mathbf{x}_1,\mathbf{x}_2;\tau,\mathbf{s})}{\partial s(n)} = -\frac{\sqrt{2}}{\sigma_v}\left(\frac{x_1(n)-s(n)}{|x_1(n)-s(n)|}+\frac{x_2(n+\tau)-s(n)}{|x_2(n+\tau)-s(n)|}\right) = -\frac{\sqrt{2}}{\sigma_v}\left[\text{sgn}\big(x_1(n)-s(n)\big)+\text{sgn}\big(x_2(n+\tau)-s(n)\big)\right], \tag{30}$$

which when set to zero, results in the following estimator

$$\hat{s}(n;\tau) = \text{med}\big\{x_1(n),x_2(n+\tau)\big\} = \frac{x_1(n)+x_2(n+\tau)}{2}. \tag{31}$$

Inserting $\hat{s}(n;\tau)$ into the log-likelihood function in (29) and maximizing with respect to the other parameter τ, we obtain

$$\hat{\tau} = \arg\min_{\tau}\sum_{\text{n}=0}^{\text{N}-1}\left(\frac{|\text{x}_1(\text{n})-\text{x}_2(\text{n}+\tau)|}{2}+\frac{|\text{x}_2(\text{n})-\text{x}_1(\text{n}-\tau)|}{2}\right). \tag{32}$$

Making use of the assumption that $s(n)$ has constant value at the extremes of the observation interval for a period larger than τ, the ML estimator of τ for Laplacian noise can be written as

$$\hat{\tau}^{\text{L}} = \arg\min_{\tau}\sum_{n=0}^{N-1}\big|x_1(n)-x_2(n+\tau)\big|, \tag{33}$$

which does not need any correction as in the Gaussian case. Expressing it in terms of the QT series, it becomes the following estimator at each j-th HR change

$$\hat{\tau}_j^{\text{L}} = \arg\min_{\tau}\sum_{n=n_{j,o}}^{n_{j,e}}\big|d_{\text{QT}}^i(n)-d_{\text{QT}}(n+\tau)\big|;\ \ \tau\in\{-I,...,I\}. \tag{34}$$

G. Evaluation in simulation of QT-adaptation time estimators

To assess the time delay estimators in simulation, we generated a QT slope corresponding to HR accelerations including a gradual ramp-like transition defined as:

$$s(n) = \begin{cases} a+b, & n=0,...,\frac{D-T}{2}-1 \\ a\left(1-\frac{2}{T+1}\left(n-\frac{D-T-2}{2}\right)\right)+b & n=\frac{D-T}{2},...,\frac{D+T}{2}-1 \\ -a+b, & n=\frac{D+T}{2},...,D-1 \end{cases} \tag{35}$$

where T takes values from a uniform random distribution between values corresponding to 10 and 70 s. The amplitude of the step is $2a$, the value at the middle of the transition step is b implying $b+a$ indicates the departing level of the step and $b-a$ the arrival one (Fig.5). In case of HR deceleration (positive slope transition in $d_{\text{QT}}(n)$) the step like transition has the form $-s(n)$. The observation signal length in samples D is taken as corresponding to 1000 s. Added white noise $v_i(n)$ was scaled to better match the variability of the real series with a factor taken randomly between 0.010 s and 0.50 s. The transition ramp $2a$ amplitude was chosen to match the amplitude range of real QT transitions. The mean stationary QT value at higher HR, $b-a$, was generated randomly between 0.23 s and 0.30 s, and at lower HR, $b+a$, between 0.33 s and 0.40 s. The simulated time lag τ was also randomly selected and ranged between 0 s and 70 s. In total, 800 series realizations, sampled at 4 Hz, were generated, which were the result of adding Gaussian/Laplacian noise to 200 realizations from each combination of negative/positive slope transition. Ranges of parameters were chosen based on real observed QT changes in stress test [13].

To evaluate the time-delay estimator's performance, the error, ε, between the true τ introduced at the simulation and the estimated one, $\hat{\tau}$, was computed as $\varepsilon = \hat{\tau}-\tau$, including superindexes to denote each particular detector, see Table II.

H. QT-adaptation-time lag in athletes

Time delay was estimated from HR accelerations when the athlete is exercising and identified with τ_a, and from HR decelerations when the athlete is recovering and identified with τ_d. A extra of 10 s, $I=40$ samples, were added at the observation interval extremes to guarantee the presence of stationary HR samples as required by the assumptions of time-delay estimators.

The presence of an observable HR transition does not guarantee the presence of an observable transition in d_{QT} and d_{QT}^i series. The d_{QT} series is characterized by a lower range of variations and higher variability than d_{RR}, which could mask the low-amplitude transitions in d_{QT} and consequently bias the estimation of transitions in d_{QT}^i. Thus, once HR transitions are identified, the analyzable transitions in d_{QT} and d_{QT}^i series were selected based on their variability. The transition is eligible for time delay computation if the global variance along the entire transition is more than three times the local variance, computed over the consecutive 10s-long windows composing the transition.

Each recording could be characterized by a total of J_a HR accelerations and J_d HR decelerations with each corresponding set of $\hat{\tau}_{j,a}$, $j\in\{1,\ldots,J_a\}$, and $\hat{\tau}_{j,d}$, $j\in\{1,\ldots,J_d\}$, de-

lay estimates. Thus a median value of $\hat{\tau}_{j,a}$, $\hat{\tau}_a^m = \text{med}\{\hat{\tau}_{j,a}\}$, and of $\hat{\tau}_{j,d}$, $\hat{\tau}_d^m = \text{med}\{\hat{\tau}_{j,d}\}$, were computed to characterize the time delay at each training session.

I. Statistical analysis

The estimated time delay τ in athletes was categorized based on sex, sports type, maximum HR reached during exercise and exercise intensity. Sports type is defined depending on the prevalence of dynamic (cycling, jogging, middle distance race, running) or static components (aerial silks, basketball, CrossFit, fitness, tennis) based on the Task force for sport classification [27]. Maximum HR (HR_m) is categorized as overcoming/no overcoming the theoretical maximal (HR_m^{T}), defined as $\text{HR}_m^{\text{T}} = 220 - \text{age}$ in bpm [28]. Another way to estimate exercise intensity is to compute the percentage of HR reserve (HRR). The HRR is the theoretical maximal HR (or the highest observed HR reached during physical activity when it is higher than the theoretical maximal HR) minus the HR at baseline. The percentage of HRR (%HRR) used during physical activity, or exercise intensity, is the ratio of the observed maximal HR minus the basal relative to HRR. Sport intensity was considered submaximal if %HRR$<$90% and maximal/near to maximal if %HRR$\geq$90%.

Normality of distributions was tested with Lilliefors test and then classes of median delays estimated from HR accelerations (τ_a^m) and HR decelerations (τ_d^m) were compared with a Wilcoxon ranksum test.

The correlation between the delays estimated from each HR accelerations ($\hat{\tau}_a$) and HR decelerations ($\hat{\tau}_d$) and the characteristics of the corresponding HR transition was computed. Each HR acceleration/deceleration was characterized in terms of duration (D_a/D_d), amplitude (A_a/A_d) computed as the difference between the minimum and maximum values of the HR transition, and slope (S_a/S_d) which is the ratio A_a to D_a and A_d to D_d.

IV. Results

A. Evaluation in simulation of QT-adaptation time estimators

An example of simulated QT transitions is shown in Fig 5. Table II contains the distribution, mean$\pm$standard deviation (SD), of $\hat{\tau}$ and relative errors ε in simulation for the different estimators under test.

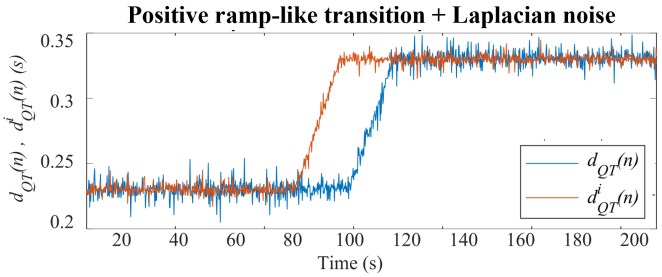

Fig. 5: Simulated QT series with linearly gradual transitions.

TABLE II: Simulation results: mean $\pm$ SD of the estimated delays $\hat{\tau}$ and errors ε distributions, reported in s.

Noise PDF	Gaussian	Laplacian
τ	21.47 ± 16.27	
$\hat{\tau}^{\text{CC}}$	21.53 ± 16.21	21.50 ± 16.21
ε^{CC}	0.06 ± 1.34	0.03 ± 1.22
$\hat{\tau}^{\text{LS}}$	21.54 ± 16.26	21.50 ± 16.29
ε^{LS}	0.07 ± 1.20	0.02 ± 1.01
$\hat{\tau}^{\text{L}}$	21.55 ± 16.18	21.48 ± 16.29
ε^{L}	0.08 ± 1.20	0.01 ± 0.90

B. QT-adaptation-time lag in athletes

Starting from the 112 ECG-signal sets belonging to healthy athletes, 62 of them were excluded due to low SNR or because belonging to the same subject, resulting in a total of 50 ECG signal sets included in the analysis, see number distribution across sports in Table I. The 50 healthy subjects are competitive or not competitive athletes with an average training rate of 4 times per week for their main sport activity. The main information of databases before and after ECGs exclusion is reported in Table III. None of the 50 subjects had previous history of cardiorespiratory diseases neither were taking drugs at the time of ECG acquisition.

A subject practicing jogging with asymptomatic SQTS was reported as case study. The subject has 2 analyzable ECGs following the exclusion criteria (refer to III-B and III-H) [19]. The subject is male and 56 years old [19].

TABLE III: Demographic and anthropocentric information of the databases SPDB and SPDB2, and of the included athletes. Missing information is reported into parenthesis. The baseline HR (HR_r), the maximal HR during physical activity (HR_m), the theoretical maximal HR (HR_m^T) and the percentage of HR reserve ($\%HRR$) were computed and reported only for the athletes included in the analysis.

Parameter	SPDB	SPDB2	Included athletes
Sex M/F	53 / 28 (0)	19 / 3 (0)	42 / 8 (0)
Age y	30 ± 13 (1)	27 ± 13 (0)	26 ± 8 (0)
Weight kg	71 ± 21 (8)	69 ± 6 (12)	69 ± 9 (5)
Height cm	170 ± 30 (8)	177 ± 6 (12)	177 ± 7 (5)
BMI kg/m^2	22.3 ± 3.5 (8)	21.7 ± 1.4 (12)	22.1 ± 2.2 (5)
Smoking NO/YES	39 / 29 (13)	18 / 4 (0)	31 / 17 (2)
HR_r (bpm)	-	-	70 [63-86]
HR_m (bpm)	-	-	190 [179-200]
HR_m^T (bpm)	-	-	197 [193-199]
%HRR (%)	-	-	95 [89-100]

The percentage, median[range] across subjects, of missing values that were linearly interpolated in the RR series is 1.8[0.6-3.7]% and in the QT series is 14.1[10.8-21.4]%.

The hypothesis of a better suitability of the Laplacian over the Gaussian time delay estimator between $d_{\text{QT}}(n)$

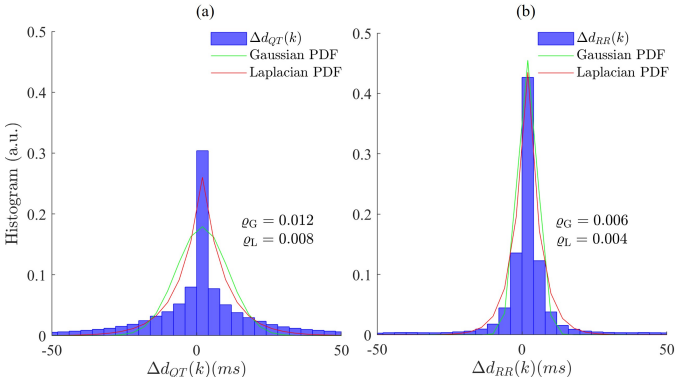

Fig. 6: The histograms of $\Delta d_{\mathrm{QT}}(k)$ and $\Delta d_{\mathrm{RR}}(k)$, displayed together with the best fit of the Gaussian and Laplacian PDFs obtained by maximizing the respective likelihood functions. Fitting errors ϱ are overprinted.

and $d^i_{\mathrm{QT}}(n)$ was evaluated analyzing the actual QT-interval variability which lead to $v_2(n)$, in (17). The median value $\bar{d}_{\mathrm{QT}}$ of consecutive five beat sets is subtracted and the resulting $\Delta_{\mathrm{QT}}(k) = d_{\mathrm{QT}}(k) - \bar{d}_{\mathrm{QT}}$ values are plotted in a histogram (Fig. 6(a)) as an estimate of the probability distribution of $v_2(n)$. This distribution is fitted with its best Laplacian and Gaussian PDF, overprinted in Fig. 6(a). Goodness of fit is quantified by the root mean squared errors, ϱ, of the PDF fitting. The Laplacian error, $\varrho_{\mathrm{L}} = 0.008$, results a 33% lower than the Gaussian, $\varrho_{\mathrm{G}} = 0.012$. When repeating the analysis for the outlier rejected plus interpolated QT series, $\Delta_{\mathrm{QT}}(n) = d_{\mathrm{QT}}(n) - \bar{d}_{\mathrm{QT}}$ same conclusion is reached, $\varrho_{\mathrm{L}} = 0.012$ and $\varrho_{\mathrm{G}} = 0.020$, corroborating the better adequacy of Laplacian distribution in the model in (17).

Analogously, the hypothesis that the RR intervals follows a Laplacian distribution, as assumed in (8), is tested and the results are displayed in Fig. 6(b) where it is evident that the Laplacian distribution provides a more accurate fit for the RR intervals compared with the Gaussian distribution.

Table IV presents the distributions of the estimated model parameters α and β in (5), error ϵ for the healthy subjects and for the SQTS subject. Table V contains the distribution of HR-transition duration (D_a and D_d), HR-transition amplitude (A_a and A_d), HR-transition slope (S_a and S_d) plus the delays $\hat{\tau}_a$ and $\hat{\tau}_d$, and $\hat{\tau}^m_a$ and $\hat{\tau}^m_d$, for each HR acceleration and deceleration. The Table VI contains the correlation coefficient between HR-transition characteristics and delays τ_a and τ_d for the healthy subjects. The SQTS subject has two analyzable signals. The $\hat{\tau}^m_a$ is 2.8 and 19.3; the $\hat{\tau}^m_d$ is 11.8 and 19.1.

An example of estimated $d^i_{QT}(n)$ series for a subject practicing running is shown in Fig. 7.

TABLE IV: Distribution (median [25^{th}-75^{th}]) of $\hat{\alpha}$, $\hat{\beta}$, ϵ for healthy athletes (H) and the subject with SQTS.

Subject	$\hat{\alpha}$	$\hat{\beta}$	ϵ (ms)
H	0.14 [0.11-0.16]	0.39 [0.37-0.42]	11 [9-16]
SQTS	0.13 [0.08-0.22]	0.44 [0.40-0.46]	11 [8-15]

Fig. 8 shows the distributions of $\hat{\tau}^m_a$ and $\hat{\tau}^m_d$ for healthy subjects categorized based on sex, sport type, HR_m, and exercise intensity along with the statistical differences from Wilcoxon ranksum test. As a result of the inclusion criteria for ramp selection presented in section III-H, the number of QT series with analyzable HR-acceleration ramp is 48 distributed as follows: 8 female, 40 male; 24 dynamic sport, 24 static sport; 31 $\mathrm{HR}_m \leq \mathrm{HR}^T_m$, 17 $\mathrm{HR}_m > \mathrm{HR}^T_m$; 6 submaximal exercise intensity, 42 maximal/ near to maximal exercise intensity. The number of QT series with analyzable HR-deceleration ramp is 39 distributed as follows: 8 female, 31 male; 19 dynamic sport, 20 static sport; 26 $\mathrm{HR}_m \leq \mathrm{HR}^T_m$, 13 $\mathrm{HR}_m > \mathrm{HR}^T_m$; 5 submaximal exercise intensity, 34 maximal/ near to maximal exercise intensity.

V. Discussion

The present work aims to characterize the time delay of QT-interval accommodation to HR accelerations and decelerations for a healthy trained population during training.

This analysis requires the computation of RR series and QT series from ECGs acquired during sports practice through wearable devices. The delineation of the ECG, and in particular of the T-wave end is negatively affected by the sport-related noise and artifacts. Eventually, T wave and P wave can overlap at very high HR. In order to improve the delineation of ECG-waves fiducial points and consequently the QT series, ECGs were only considered for analysis if 65% of the signal has acceptable values of $\mathrm{SNR}_{\mathrm{HF}}$ and $\mathrm{SNR}_{\mathrm{LF}}$. In addition the identification of ECG-wave onsets and ends was visually checked and segments with large false negative detection were further subsegmented for artifact exclusion and reannotated. Further, even if the ECG is acceptable, the dynamics of the QT interval was not studied in windows where $\mathrm{SNR}_{\mathrm{HF}}$ and $\mathrm{SNR}_{\mathrm{LF}}$ are under the threshold. Possible sources of artifacts and data loss are that the conductive sensor pads were not humidified enough to increase conductivity or the chest band was not tight enough to maximize the contact with the body and minimize its movement. Furthermore, we can imagine that athletes who made extreme efforts may have ECG signals corrupted by high baseline wandering due to heavy respiration and body movement. Even if the ECG selection based on the SNR may have excluded a high number of recordings, the number of analysed ECGs is necessarily reduced to guarantee a reliable analysis, especially for the computation of the QT interval. The accuracy of QT measurements directly depends on the ability to accurately determine the QRS onset and T end. The T-end determination is challenging, especially in the presence of high levels of noise. The localization of wave onsets and ends is much more difficult, as the signal amplitude is low at the wave boundaries and the noise level can be higher than the signal itself. Of note, there is not any universally acknowledged rule to locate the end of the T wave. In literature, very different delineation approaches are present based on mathematical models, derivative curve, ECG slope criteria, the wavelet transform, adaptive filtering, artificial neural networks, hidden Markov models, support vector machine, partially collapsed Gibbs sample and Bayesian,

This article has been accepted for publication in IEEE Transactions on Biomedical Engineering. This is the author's version which has not been fully edited and content may change prior to final publication. Citation information: DOI 10.1109/TBME.2024.3505417

TABLE V: Distribution (median [25^{th}-75^{th}]) of HR-transition duration (D), HR-transition amplitude (A), HR-transition slope (S), $\hat{\tau}$, $\hat{\tau}^m$ in HR accelerations (sub-index "a") and decelerations (sub-index "d") for healthy athletes (H).

Subject	D_a (s)	A_a (s)	S_a (%)	$\hat{\tau}_a$ (s)	$\hat{\tau}_a^m$ (s)	D_d (s)	A_d (s)	S_d (%)	$\hat{\tau}_d$ (s)	$\hat{\tau}_d^m$ (s)
H	36.3 [27.0-45.3]	1.5 [1.0-2.6]	0.4 [0.3-0.7]	4.3 [0-11.3]	6.8 [2.1-15.0]	37.3 [24.8-53.8]	1.3 [0.9-1.9]	0.4 [0.2-0.5]	8.3 [1.3-16.0]	8.8 [5.3-16.9]

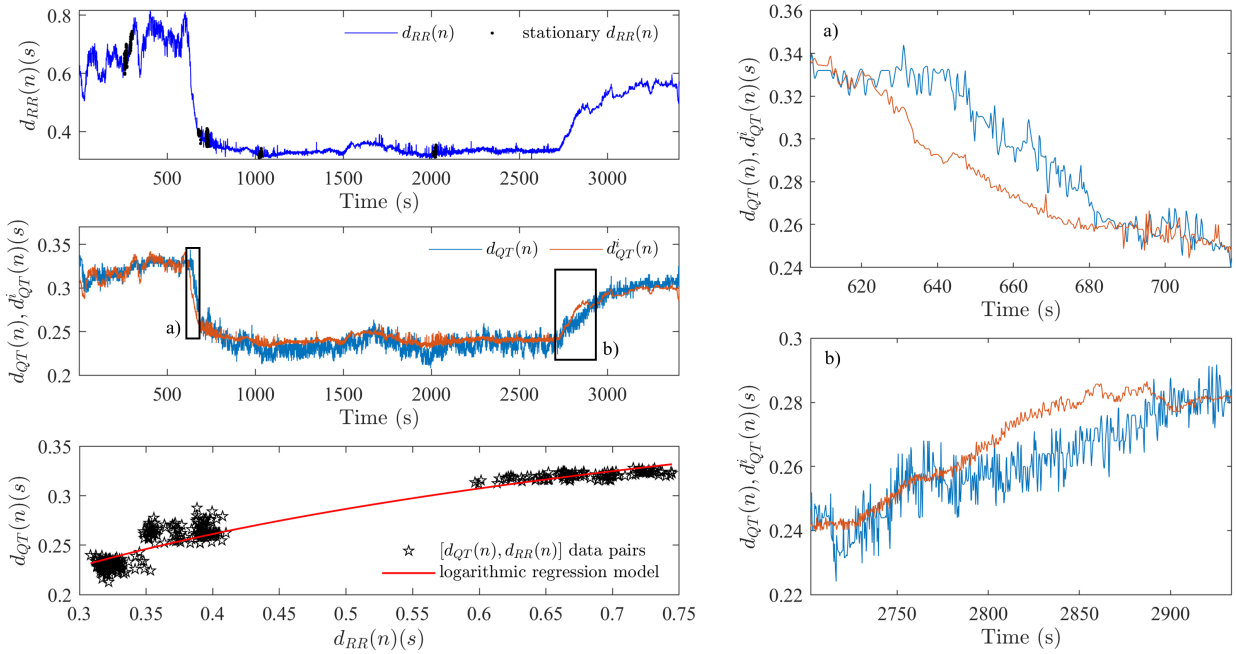

Fig. 7: Estimation of expected instantaneous memoryless, HR-dependent, QT-interval series $d^i_{\mathrm{QT}}(n)$ through a logarithmic regression model from an ECG recording acquired during running. On the left side, the first row shows $d_{\mathrm{RR}}(n)$ and its selected stationary windows marked in black. The second row shows the estimated $d^i_{\mathrm{QT}}(n)$ overlapped with $d_{\mathrm{QT}}(n)$ where a delay between them can be appreciated at the large HR transitions (zoom presented in panel a) and b)). The third row shows the logarithmic model fitting data pairs of $d_{\mathrm{RR}}(n)$ and $d_{\mathrm{QT}}(n)$ in stationary windows.

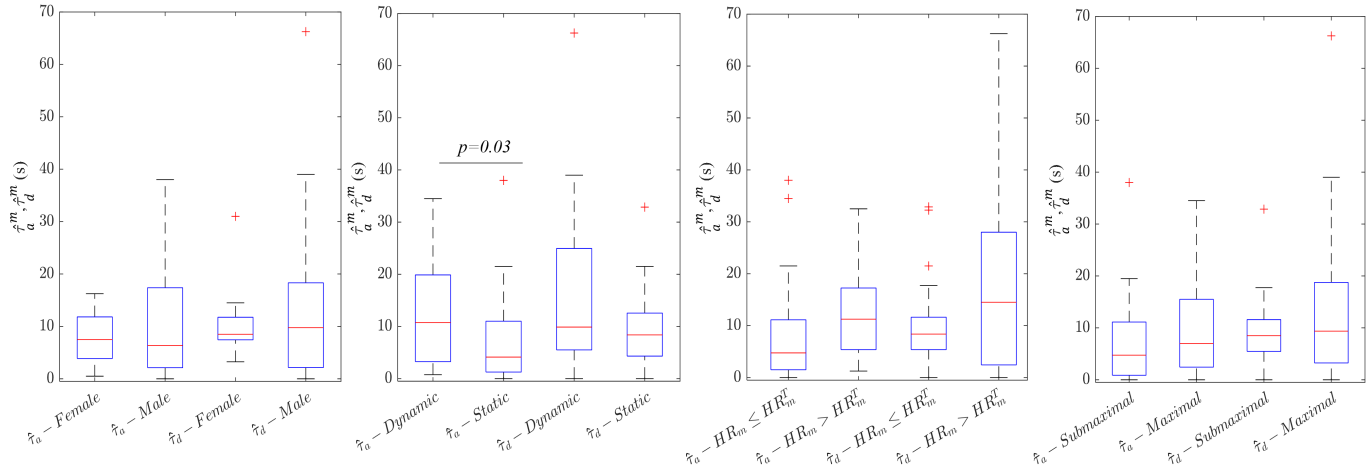

Fig. 8: Boxplot of distribution of τ_a^m and τ_d^m for healthy athletes when categorized for sex, sport type, HR_m reached during exercise and exercise intensity.

TABLE VI: Correlation coefficient between HR-transition characteristics and estimated delays $\hat{\tau}_a$ and $\hat{\tau}_d$ for the healthy subjects. * significance of correlation $p < 0.05$

τ/HR-transition	D_a	A_a	S_a	D_d	A_d	S_d
$\hat{\tau}_a$	0.10	-0.11	-0.24*	-	-	-
$\hat{\tau}_d$	-	-	-	0.30*	0.10	-0.17*

"wings" function, TU complex analyses, correlation analysis, and k-nearest neighbor [29]. Among them, the wavelet-based delineator used here is one of the commonly applied for T-end detection [21]. Furthermore, the QT interval is lead dependent, as all ECG parameters are. This is caused by the varying projections on different lead vector axes. Historically,

measurement of QT intervals has been preferably performed in lead II. When the T wave is not easily identified in lead II, lead V5, V6 or I can be alternatively used [30]. Other authors suggest to derive the QT interval by computing the median of QT intervals from a total of 6 leads with 3 leads taken from peripheral leads (avoiding III and aVR because of frequent low voltages and inverted polarity, respectively) and 3 precordial leads (preferably V2, V4, and V6) [31]. Alternatively, the QT interval can be computed in a lead derived from the Principal Component Analysis (PCA), losing the dependency of ECG measurements on the specific ECG lead. The latest approach was used to compute the QT/RR hysteresis during stress tests from patients with suspected cardiovascular disease [13]. The present work computes the QT interval in a single-lead ECG acquired from a chest band, whose conductive ECG sensor pads are located at the centre of the thorax and the midaxillary line, resulting in a pseudo-V6 lead, typically used to compute the QT interval. Due to only having a single lead available, the spatial dispersion over leads of the length and hysteresis of the QT interval could not be evaluated in this work.

In the computation of RR and QT series, a piecewise cubic Hermite polynomial is used to uniformly interpolate the RR and QT series, since piecewise cubic Hermite polynomial avoids the generation of high amplitude spikes and series overestimation when there are longer portion of data loss or artifacts [32]. This enables a more reliable signal processing than classical cubic spline interpolation [32].

The relation between HR acceleration/deceleration and their induced QT changes has been modelled with a transformation part (typically non-linear), representing the stationary relation of QT with RR, plus a first order linear system representing the system memory [33]. First of all, the transformation relation was applied to obtain the instantaneous memoryless HR-dependent QT-interval series, because the time delay between $d_{\mathrm{QT}}(n)$ and $d_{\mathrm{RR}}(n)$ cannot be estimated directly due to the different range of amplitudes [13]. In order to estimate the model parameters of the transformation relation between QT and RR, six stationary windows of which mean RR is closest to the maximum, minimum and mean (two windows from each condition) value of $d_{\mathrm{RR}}(n)$ were considered. Stationary windows guarantee that the dominant dependency between RR and QT is mostly the transformation part, so excluding the first order linear system part representing the system memory, and favoring a proper estimation of parameters α and β representative of the instantaneous transformation part. However, the stationarity of those windows can not be really guaranteed during real-case training, mainly due to movement and concurring artifacts. Thus, athletes may be advised to have complementary standard ECGs acquired during clinical stress tests with better stationary conditions to estimate the model parameters α and β. This is possible since QT-RR relationship pattern exhibits intra-subject stability (refer to Fig. 4 of Supplementary Materials) [34]. Conversely, the QT/RR relation is different between different subjects (refer to Fig. 1, 2, 3 of Supplementary material). However, the SQTS subject presents less stability in the QT/RR relation (refer to Fig. 5 in the Supplementary Material).

Abrupt acceleration and deceleration in $d_{\mathrm{RR}}(n)$ were automatically detected by a GLRT-based algorithm. In the GLRT-based algorithm, the parameter *T*, representing the duration of the HR change, was taken corresponding to $30s$ because it is the average transition length observed in our dataset. Abrupt changes in RR series could alternatively had been identified by visual inspection and manual annotation, based on the evident change in RR series slope and variability. However, these manual annotations would be highly subjective, time-consuming and laborious [35]. Therefore, the automatic identification here presented is preferred, which if desired can be afterwards manually supervised.

The superior adequacy of the Laplacian modeling of QT variability was already shown true in a study where delay was estimated both in simulation and in clinical stress tests for coronary artery disease stratification [18]. The present study confirmed that variability in the features derived from the ECG as the RR interval $d_{\mathrm{RR}}(k)$ and QT interval $d_{\mathrm{QT}}(k)$ is better represented by Laplacian distribution than Gaussian (Fig. 6). Indeed, electrocardiographic measures as the QT interval, based on QRS-onset and T-end identifications, are largely subjected to outliers when ECGs are acquired in highly noisy conditions during training [18]. The same study is repeated for RR-interval and QT-interval characterization after outlier rejection plus interpolation, $d_{\mathrm{RR}}(n)$ $d_{\mathrm{QT}}(n)$ respectively, obtaining similar results and confirming that Laplacian distribution assumption in (17) is more adequate than Gaussian.

Maximum likelihood detectors of the QT-adaptation-time lag have been derived based on Gaussian and Laplacian noise assumptions. The simulation results show that both Gaussian and Laplacian noise distribution based estimators slightly overestimate τ in case both of Gaussian noise and of Laplacian noise (Table II). In the case of Gaussian noise, the best-performing estimator is τ^{LS}, with an error SD of $\varepsilon^{\mathrm{LS}}$ of 1.20 s while τ^{CC} gives the highest SD of $\varepsilon^{\mathrm{CC}}$ of 1.34 s. The lower performance of τ^{CC} could be a result of the extra variance added by the estimation of the extra parameter and b. In case of Laplacian noise, the best-performing estimator is τ^{L} with SD of ε^{L} of 0.90 s [18]. The estimators $\varepsilon^{\mathrm{LS}}$ and ε^{L} were clinically tested estimating the time delay in stress test of patients with coronary artery diseases. During this evaluation, the ε^{L} shows superior adequacy for time-lag estimation [18]. Given the previous results and the fact that the distribution of the QT series has shown to be closer to Laplacian PDF distribution, the τ^{L} appears as the detector of choice, and is the one used in the actual data analysis.

The time-lag estimates in the athletes population showed that $\hat{\tau}_a^m$ is on average lower than $\hat{\tau}_d^m$, which is compatible with an increment of repolarization dispersion after the large increase in sympathetic activity reported in exercise and emotions [15]. This difference between the QT-interval delay during HR acceleration versus deceleration had been already shown during incremental pacing manoeuvres[9], which are representative for the QT/RR relation during physical activity, and when provoked by atropine bolus injection [16].

Female athletes have slightly but not significantly lower time delays than male athletes. This is compatible with a previous study, in which the speed of QT/RR hysteresis was found to be faster in females than in males [36]. However,

results could be biased by the unbalanced population. Categorizing by sport type, dynamic sports present higher $\hat{\tau}_a^m$ and $\hat{\tau}_d^m$ than static activities. Categorizing by HR_m, $\hat{\tau}_a^m$ and $\hat{\tau}_d^m$ are higher when $\mathrm{HR}_m > \mathrm{HR}_m^{\mathrm{T}}$ than when $\mathrm{HR}_m \leq \mathrm{HR}_m^{\mathrm{T}}$. Dynamic activities and $\mathrm{HR}_m > \mathrm{HR}_m^{\mathrm{T}}$ are eventually linked with higher physical exertion which may be linked to increased repolarization dispersion. Another way to characterize exercise intensity is the percentage of HRR used. The number of subjects that are at the maximal or near to maximal exertion increases with this metric with respect to the classification based on the HR_m^T. Nonetheless, the conclusions do not change and those subjects that are in the maximal zone exhibit a higher time delay on average than the subjects who trained in the submaximal zone of HR.

However, a direct relationship between prolonged QT memory with arrhythmias can not be established. The cardiac electrical activity and the development of arrhythmias can depend on several elements after exercise. Firstly, there are several metabolic alterations that last after cessation of physical activity and might contribute to arrhythmia development, e.g. excessive catecholamines release [37]. Another factor can be the exercise-related adaptations in the cardiac autonomic modulation as well as the other structural, electrical and functional adaptations of the athlete's heart [38].

The estimated delay does not correlate (in three cases significantly) with the duration, the amplitude and the slope of the HR acceleration and deceleration.

For completeness, the time delay of the pathological subject with SQTS and practicing jogging was analysed. In short QT syndrome, the repolarization heterogeneity as well as the abnormal QT-RR relationship is more pronounced at lower HR, and QT intervals characteristically show lack of adaptation to HR changes [39]. $\hat{\tau}_d^m$ is greater than the corresponding delays for the healthy population. This result could be justified by the shorter QT interval in SQTS subjects as compared to healthy people at corresponding RR. Remarkably greater $\hat{\tau}_d^m$ could be explained by the phenomenon of deceleration-dependent shortening of QT interval (shortening of QT interval associated with a decrease in HR) caused by strong parasympathetic stimuli [39]. The SQTS subject seems to have greater variability in the estimation of model parameter α than healthy subjects. Although, this is only one subject and the inferred observations remain subject of debate, studies with a considerable population of SQTS subjects still involved in sports practice are needed to confirm them.

The QT-adaptation time values obtained for sport athletes, and reported in Table V, are remarkably lower in mean than those reported in other populations during stress tests as in [13], [40]. This can be due to age populations differences across studies. However, it can also be that the methodology here presented to estimate the τ result in negatively biased estimates when the HR excursion of the transition are low, as it is in our data [15].

Finally, is worth to mention that QT hysteresis is a physiological adaptation mechanism which may also reflect the timing differences of this process in various regions of the ventricles. However, it is still unclear how this contributes to the risk of arrhythmias.

VI. Limitation and future improvement

The athletic population used in this study is unbalanced in terms of sex and age, future works should aim to collect ECGs during training in female and old athletes to further investigate the relation of QT/RR hysteresis with sex and age. Despite the current database has served for the development of the algorithm, future databases are needed for performance evaluation of the presented algorithm.

The delineation of the T-wave end is challenging and less accurate than the detection of the T-wave peak. Future studies can be designed to separately evaluate the adaptation of the early and late parts of the repolarization, in order to understand if the QT_{peak} interval is not only more robust, but also equivalent to characterize the repolarization adaptation in pathological scenario.

Further, as required by the formulation of the time delay estimator, an interval of length I (in this work 10s) at the observation interval onset and end was added to guarantee the presence of stationary HR samples. However, changes in sympatho-vagal activation occur as approaching the extremes of abrupt HR changes as well as during the different phases of exercise. These changes in sympatho-vagal activation affects the time delay resulting in the fact that it is not constant along the duration of the ramp [41]. Furthermore, the ramp-like transition may not represent accurately the extremes of an HR acceleration or deceleration. A specific study on the relation of time delay and HR-transition duration/phases may be designed to explore this effect.

In addition, the QT-adaptation time lag, is known to be composed of two phases: one initial fast adaptation phase lasting a few seconds followed by a slow adaptation phase with a time constant of more than 30 seconds [7], [14]. These two phases have not been considered separately, so the estimated time delay is expected to be the one of a single exponential fitting the two phases. Future works should explore the possibility to obtain independent estimators for each phase time constant.

On the clinical applications side, the study does not allow to establish the clinical value of the biomarker in a sports practitioner population. To study this potential value, studies need to be conducted where knowledge exists, or can be derived by other techniques, about the SCD risk of the involved subjects, and then threshold values on τ for triggering risk alarm could be inferred from them. One possible approach can be to involve a matching population of SCD survivors with implanted ICD still engaged in sports. The comparison between SCD survivors and the healthy subjects can elucidate whether their QT-RR dynamics can discriminate between different level of arrhythmic risk. This approach should be implemented with a standard clinical exercise tests that can guarantee better acquisition conditions and delete the spontaneous behaviours introduced by many different types of sport.

VII. Conclusion

A method to compute the QT lag in response to HR changes from ECGs acquired through wearable sensors while practicing sports has been proposed. The method includes

identification of HR changes episodes, done with a GLRT detector of linear transition HR ramps, and a Maximum Likelihood QT time delay estimator based on Laplacian noise distribution. The Laplacian estimator has been proven to be superior to those based on Gaussian distributions.

As expected, the QT-adaptation time-lag estimated during HR deceleration, especially after intense physical exertion of athletes, is characterized by longer time delays than during HR acceleration. The difference between the hysteresis/delay of QT adaptation to HR deceleration versus acceleration is of smaller magnitude than at supine rest, which is what would be expected as a result of higher sympathetic activation at sport.

The proposed method to measure the QT memory time lag opens an opportunity to monitor the cardiac activity during real exercise and consequently to understand what happens in cardiac electrophysiology during physical activity when malignant arrhythmogenic events may occur, especially in subjects with congenital or structural heart disease.

ACKNOWLEDGMENT

This work was funded by projects TED2021-130459B-I00 and PID2022-140556OB-I00, MICINN Spanish and FEDER, and BSICoS Group-T39-23R, by Gobierno de Aragon.

REFERENCES

[1] A.G. Yow et al. (2024, Mar.). Sudden cardiac death. *Treasure Island (FL): StatPearls Publishing*. [Online]. Available: https://www.ncbi.nlm.nih.gov/books/NBK507854/

[2] J. Han et al., "Sudden cardiac death in athletes: Facts and fallacies," *J Cardiovasc Dev Dis.*, vol. 10, no. 68, Feb. 2023.

[3] G. Finocchiaro et al., "Sudden cardiac death in young athletes: JACC state-of-the-art review," *J Am Coll Cardiol.*, vol. 16, no. 83, pp. 350–370, Jan. 2024.

[4] S. Romagnoli et al., "Initial investigation of athletes' electrocardiograms acquired by wearable sensors during the pre-exercise phase," *Open Biomed Eng J*, vol. 15, pp. 37–44, Jul. 2021.

[5] P. Laguna et al., "Techniques for ventricular repolarization instability assessment from the ECG," in *P*roceedings of the IEEE, vol. 104, no. 2, pp. 392–415, Feb. 2016.

[6] N.V. Arteyeva, "Dispersion of ventricular repolarization: Temporal and spatial," *World J. Cardiol*, vol. 12, no. 9, pp. 437–449, Sep. 2020.

[7] K. J. Axelsson et al., "Adaptation of ventricular repolarization duration and dispersion during changes in heart rate induced by atrial stimulation," *Ann Noninvasive Electrocardiol*, vol. 25, no. 3, e12713, May 2020.

[8] R. Ang and N. Marina, "Low-frequency oscillations in cardiac sympathetic neuronal activity," *Frontiers in physiology*, vol. 11, 236, Mar. 2020.

[9] A. Hernandez-Vicente et al., "ECG ventricular repolarization dynamics during exercise: temporal profile, relation to heart rate variability and effects of age and physical health," *Int. J. Environ. Res. Public Health*, vol. 18, 9497, Sep. 2021.

[10] C. Pérez et al., "Characterization of impaired ventricular repolarization by quantification of QT delayed response to heart rate changes in stress tests," in *Proc. IEEE Comput. Cardiol.*, 2020, pp. 1–4.

[11] E. Pueyo et al., "Characterization of QT-interval adaptation to RR interval changes and its use as a risk-stratifier of arrhythmic mortality in amiodarone-treated survivors of acute myocardial infarction," *IEEE. Trans. Biomed. Eng.*, vol. 51, no. 9, pp. 1511–1520, Sep. 2004.

[12] H. Gravel et al., "Clinical applications of QT/RR hysteresis assessment: a systematic review," *Ann Noninvasive Electrocardiol.*, vol. 23, no. 1, e12514, Jan. 2018.

[13] C. Pérez et al., "QT-interval time lag in response to heart rate changes during stress tests for Coronary Artery Disease diagnosis," *Biomedical Signal Processing and Control*, vol. 86, 105056, Jan. 2023.

[14] A. Cabasson et al., "Estimation and modeling of QT-interval adaptation to heart rate changes," *IEEE Trans Biomed Eng.*, vol. 59, 956–965, Apr. 2012.

[15] H. H. M. Draisma et al., "Increased dispersion of ventricular repolarization during recovery from exercise", in *Proc. IEEE Comput. Cardiol.*, 2005, vol. 32, pp. 85–88.

[16] K. J. Axelsson et al., "Adaptation of ventricular repolarization time following abrupt changes in heart rate: comparisons and reproducibility of repeated atrial and ventricular pacing," *Am J Physiol Heart Circ Physiol.*, vol. 320, pp. H381–H392, Jan. 2021.

[17] C. Pérez et al., "Performance evaluation of QT-RR adaptation time-lag estimation in exercise stress testing," *IEEE Trans Bim. Eng.*, v. 5, 2024.

[18] S. Romagnoli et al., "Model-based estimators of QT series time delay in following heart-rate changes," in *Annu Int Conf IEEE Eng Med Biol Soc.*, 2023, pp. 1-4.

[19] A. Sbrollini et al., "Sport Database: Cardiorespiratory data acquired through wearable sensors while practicing sports," *Data in Brief*, vol. 27, 104793, Dec. 2019.

[20] S. Romagnoli et al., "Sport DB 2.0: A New Database of Data Acquired by Wearable and Portable Devices While Practicing Sport," in *Proc. IEEE Comput. Cardiol.*, 2023, pp. 1–4.

[21] J. P. Martínez et al., "A wavelet-based ECG delineator: evaluation on standard databases," *IEEE Trans Bim. Eng.*, vol. 51, no. 4, pp. 570–581, Apr. 2004.

[22] R. Bailón et al., "A robust method for ECG-based estimation of the respiratory frequency during stress testing," *IEEE Trans Bim. Eng.*, vol. 53, no. 7, pp. 1273–1285, July 2006.

[23] R. Bailón et al., "Coronary artery disease diagnosis based on exercise electrocardiogram indexes from repolarisation, depolarisation and heart rate variability," *Med. Biol. Eng. Comput.*, vol. 41, no. 5, pp. 561–571, Sep. 2003.

[24] D. Romero et al., "Ischemia detection from morphological QRS angle changes," *Physiological Measurement*, vol. 37, pp. 1004–1023, May 2016.

[25] A. Mincholé et al., "Detection of body position changes from the ECG using a Laplacian noise model," *Biomedical Signal Processing and Control*, vol. 14, pp. 189–196, Aug. 2014.

[26] L. Sörnmo and P. Laguna, "Bioelectrical signal processing in cadiac and neurological application," *Elsevier Academic Press*, 2005.

[27] J. H. Mitchell et al., "Task Force 8: classification of sports," *J Am Coll Cardiol.*, vol. 45, pp. 1364–1367, Apr. 2005.

[28] S. M. Fox et al., "Physical activity and the prevention of coronary heart disease," *Ann Clin Res.*, vol. 3 pp. 404-–32, 1971.

[29] P-C. Su et al., "Robust T-end detection via T-end signal quality index and optimal shrinkage," *Sensors*, vol. 20, 7052, Dec. 2020.

[30] P. G. Postema and A. A. Wilde, "The measurement of the QT interval," *Curr Cardiol Rev.*, vol. 10, pp. 287–294, Aug. 2014.

[31] M. Schiavone et al., "Arrhythmogenic risk and mechanisms of QT-prolonging drugs to treat COVID-19," *Card Electrophysiol Clin.*, vol. 14, pp. 95–104, Mar. 2022.

[32] K. K. Kim et al., "The effect of missing RR-interval data on heart rate variability analysis in the frequency domain," *Physiological measurement*, vol. 30, pp. 1039-–1050, Aug. 2009.

[33] E. Pueyo et al., "Mechanisms of ventricular rate adaptation as a predictor of arrhythmic risk," *Am J Physiol Heart Circ Physiol*, vol. 298, pp. H1577–H1587, May 2010.

[34] V. N. Batchvarov et al., "QT-RR relationship in healthy subjects exhibits substantial intersubject variability and high intrasubject stability," *Am J Physiol Heart Circ Physiol.*, vol. 282, pp. H2356–H2363, June 2002.

[35] S. Romagnoli et al., "Signal processing for athletic cardiovascular monitoring with wearable sensors: Fully automatic detection of training phases from heart rate data," in *IEEE International Conference on Bioinformatics and Biomedicine*, 2021, pp. 1491–1494.

[36] I. Andršová et al., "Sex and rate change differences in QT/RR hysteresis in healthy subjects," *Frontiers in Physiology*, vol. 12, 814542, Feb. 2022.

[37] J. H. O'Keefe et al., "Potential adverse cardiovascular effects from excessive endurance exercise," *Mayo Clin Proc.*, vol. 87, pp. 587–595, Jun. 2012.

[38] H. Dores et al., "The hearts of competitive athletes: an up-to-date overview of exercise-induced cardiac adaptations," *Rev Port Cardiol.*, vol. 34, pp. 51–64, Jan. 2015.

[39] C. Patel et al., "Short QT syndrome: From bench to bedside," *Circ Arrhythm Electrophysiol.*, vol. 3, pp. 401–408, Aug. 2010.

[40] E. Pueyo et al., "A dynamic model to characterize beat-to-beat adaptation of repolarization to heart rate changes", *B*iomedical signal processing and control, vol. 3 pp. 29–43; Jan. 2008.

[41] C. Pérez et al., "The Role of β-adrenergic Stimulation in QT-interval Adaptation to Heart Rate During Stress Tests," *Plos One*, vol. 18, no. 1, e0280901, Jan. 2023.